Modelling of stand basal area from leaf and plant area indices in boreal forest systems of Sweden

Alex Appiah Mensah
Supervisor: Emma Holmström, SLU Southern Swedish Forest Research Centre

Swedish University of Agricultural Sciences
Master Thesis no. 297
Southern Swedish Forest Research Centre
Alnarp 2018

Modelling of stand basal area from leaf and plant area indices in boreal forest systems of Sweden

Alex Appiah Mensah
Supervisor: Emma Holmström, Southern Swedish Forest Research Centre, SLU
Examiner: Eric Agestam, Southern Swedish Forest Research Centre, SLU

Swedish University of Agricultural Sciences
Master Thesis no. 297
Southern Swedish Forest Research Centre
Alnarp 2018

Master thesis in Forest Science
Advanced Level (A2E), 30 ECTS, SLU course code EX0838

Abstract

Leaf or plant area index (LAI/PAI) is a useful biophysical indicator to characterize the interrelationships between forests and the atmosphere and offers greater potential to estimate productivity of forested landscapes. Recently, hemispherical photography has been used in a pilot study implemented in the Swedish National Forest Inventory (NFI) to estimate LAI. However, using this indirect approach to estimate stand basal area has been less explored in boreal forests of Sweden. This study sought to evaluate the use of LAI in estimating stand basal area for different forest structures (species composition, age, density) and site characteristics using data from the 2016 and 2017 NFI. A 10-year average of absorbed radiations and precipitation for summer months obtained from the Japanese Reanalysis-55 were used to augment a stepwise regression modeling of measured basal area for monocultures of Norway spruce, Scots pine, mixed coniferous and broad-leaved forests. Models with indirect estimates of leaf area were significant ($p < 0.001$) for all species. The explained variation was higher for models with LAI functions in Norway spruce (77 %) and Scots pine (71 %) compared to mixed coniferous (60 %) and broad-leaved forests (60 %) with general PAI estimates. Other predictors such as absorbed radiation, stand age and density contributed to the explained variations. It is evident that leaf area index could enhance current predictions of stand basal area and increase the sensitivity of these models to climate change. It is also acknowledged that spectral and textural variables from higher resolution satellite imagery and digital elevation models would substantially improve the model estimates of basal area in boreal forest systems.

Keywords: Leaf plant area index, plant area index, Norway spruce, Scots pine, mixed forest, basal area, national forest inventory, Sweden.

Acknowledgements

To God be the glory for great things HE has done in my life since childhood. I owe sincere thanks and gratitude to my supervisor Dr. Emma Holmström, for her dedication and invaluable support offered me in every phase of this thesis. I also extend my sincere thanks to Prof. Urban Nilsson, Prof. Per-Magnus Ekö and Dr. Eric Agestam for their excellent lectureship on introducing me to concepts of boreal forest management in Sweden. Also, much thanks go to Martin Goude for his guidance in using CAN-EYE software and providing correction functions for leaf area index. It is also my utmost pleasure to acknowledge Desiree Mattsson for her administrative assistance and to my former course-mates of the Euroforester program, I appreciate every bit of love, ideas and friendship.

I also thank the secretariat of Erasmus Mundus program in Sustainable Forest and Nature Management for supporting my MSc thesis financially and administratively.

Also, to be acknowledged0 is the" Karl Erik Önnesjös stiftelse för vetenskaplig forskning och utveckling", which provided financial support for the LAI-equipment used in the study.

To, my lovely family in Ghana, it was through your prayers, and happy conversations that motivated me to work assiduously in my MSc studies. To my soul mate, Yvonne Adusei Yeboah, I cherish your love and encouragement in every facet of my education and social life in Europe.

Contents

Abstract *3*

Acknowledgements *4*

1 Introduction **7**

1.1 Research Questions 10

2. Materials and Methods **11**

2.1 Latitudinal gradient and forest cover description of Sweden. 11

2.2 National forest inventory design and measurement of tree and stand attributes 12

2.3. The sampling of hemispherical photographs, characterization, and processing 13

2.4 Acquisition of climate predictors for canopy attributes modelling 16

2.5 Model development and statistical data analysis 19

3. Results **23**

3.1 Estimation of leaf and plant area indices 23

3.2 Estimation of basal area from stand and site variables. 23

4. Discussion **27**

4.1 Species specific models for prediction of stand basal area from site characteristics 27

References **31**

1 Introduction

Plant area index (PAI) when referring to all light blocking elements (leaves, twigs and stems) or leaf area index (LAI), defined as half the total developed leaf area per unit of ground horizontal surface area (Chen & Black, 2006 ; Stenberg, et al., 2004), represents an important biophysical parameter to characterize exchange of energy, water vapour and carbon dioxide between terrestrial ecosystems and atmosphere (Propastin & Erasmi, 2010; Bonan, 1993). Because of this, LAI has been widely applied in ecological studies and serves as a significant input variable in many transpirational models, precipitation models and primary production models (Propastin & Erasmi, 2010; Chen et al., 1997; Johnson & Thornley, 2006). For example, Landsberg & Waring (1997), have demonstrated the usefulness of LAI in the physiological process-based model (3-PG hybrid model) in describing radiation-use efficiency, carbon balance, and partitioning. Hence, derived LAI has the potential to describe growth characteristics, canopy health (Stenberg et al., 2004) and productivity of forests (Franklin et al., 1997). Nonetheless, the performance of these models is highly sensitive to the variation of LAI at varying spatiotemporal scales and therefore requires an accurate estimation of LAI (Li, 2010).

Several approaches (direct and indirect methods) have been widely used to estimate LAI values in different landscapes across biogeographical scales (Gower, Kucharik, & Norman, 1999). Direct methods employ ground-based approaches of destructive sampling, litter fall collection and point contact sampling to determine LAI (Zheng & Moskal, 2009). Jonckheere et al. (2004) reported that direct measurement approaches give accurate values of LAI, whereas, several others argued that the approach is very costly, laborious, time-consuming and nearly impractical in large areas and for small plants in inadequate experimental plots (Propastin & Erasmi, 2010; Zheng & Moskal, 2009; Li, 2010; Gobron, Pinty, & Verstraete, 1997).

On the other hand, indirect methods of LAI estimation such as LAI optical instruments and satellite sensors have been extensively used in larger areas (Zheng & Moskal, 2009; Li, 2010) and thus, provide a timely assessment of LAI (Chen et al., 1997). Friedl et al. (1994) and Epiphanio & Huete (1995), have demonstrated the usefulness of LAI estimations using remote sensing. In addition, to abate the area-coverage estimation deficiencies associated with direct methods, remote sensing involving spectral-derived indices has proven satisfactory results

(Chen & Cihlar, 1996). Such remotely sensed techniques employ regression models and canopy reflectance model inversions to correlate LAI to band radiance or model LAI-vegetation index relation (Chen & Cihlar, 1996). Nonetheless, remotely sensed LAI-vegetation indices require ground-based observations for cross-calibration (Wang et al., 2004). The incorporation of covariates of spectral and textural variables built from high resolution satellite imageries would provide immense prospects in estimating basal area and predicting current potential site productivity. Subsequently, these site productivity estimates could be pivotal in identification and prioritization of stands for different management treatments, as well as provide new information on forest diversity and growth characteristics (Franklin et al., 1997). In addition, LAI estimates could be obtained from correlations with vegetation indices (Baret & Buis, 2008) and develop readily available LAI distribution map over varying spatial and temporal scales (Cohen, Maiersperger, Gower, & Turner, 2003).

The use of optical instruments such as LAI-2000 plant canopy analyser (LI-COR, Lincoln, Nebraska) and hemispherical photography to estimate LAI have been thoroughly investigated (Chen & Cihlar, 1995; Kucharik et al., 1997). However, other reports suggest that the use of indirect methods largely underestimate the LAI by 25 – 50 % (He, Guo, & Wilmshurst, 2007; Chason, Baldocchi, & Huston, 1991). Gower et al. (1999), attributed this problem to the non-random distribution of foliage in the canopy and radiation interception by wood elements. Usually, an assumption of randomness of foliage is used to obtain estimates of LAI values in many canopy studies using canopy gap or sky fraction primarily due to the lack of information about the randomness coefficient used in the software algorithm to compute the LAI (Gower et al., 1999). Moreover, the assumption of randomness of foliage distribution in open-canopy of boreal conifer forests (Kucharik et al., 1997; Chen et al., 1997) is invalid and such an approach could produce errors in excess of 100% (Fassnacht, Gower, Norman, & McMurtric, 1994). A likely reason is that needles of conifers are not regularly arranged in space and assuming a homogeneous canopy will systematically underestimate the canopy radiation transmittance (Chianucci & Cutini, 2012). To overcome this problem, van Gardingen, Jackson, Hernandez-Daumas, Russell, & Sharp (1999) reported that, correcting for foliage clumping can reduce underestimation by 15%.

Sampling designs represent a crucial planning tool, especially when conducting ground-based measurements that are jeered towards practical and statistical precision (Weiss, Baret, Smith, Jonckheere, & Coppin, 2004). In hemispherical photography, the number of images

and spatial location define the sampling strategy. Additionally, canopy and vegetation type, sensor angle of view, plot area and proximity to the forest-stand boundary, also affect the accuracy of the sampling design (Chason et al., 1991).

To better understand ecological processes and patterns at varying spatial scales, it is prudent to assess the accuracy of LAI values against sensitive site factors (Shen, Li, & Guo, 2014; Chen et al., 1997). Globally, LAI changes with vegetation biomes, for example, LAI is highest in tropical forest areas, moderate in agricultural landscapes, and lower LAI values recorded in desert areas (Shen et al., 2014). Kucharik et al. (1997) attributed temporal variation in LAI to seasonality. Biotic and abiotic factors largely contribute to these spatiotemporal variations of LAI. Species composition, canopy structure and phenology are crucial biotic factors that could potentially derail the accuracy of LAI estimations (Weiss et al., 2004; Hunt, Haile, Hoback, & Higley, 1999). On the other hand, abiotic variables such as temperature, radiation, topography, and soil moisture also contribute significantly to the accuracy of estimated LAI values (Weiss et al., 2004; Hunt et al., 1999).

In Sweden and many other boreal forests, differentiation in latitudinal gradients affects the distribution of tree species, soil moisture, fertility and temperature. In the northern part of Sweden, *Pinus sylvestris* (Scots pine) largely dominates the forest areas whereas the southern forest landscapes are widely covered with *Picea abies* (Norway spruce). Though there are many other tree species (*Pinus contorta*, birch, and noble broadleaves), conifers largely dominate in forest biomes across the country (Lundström and Wikberg, 2017 cited in Barreiro, Schelhaas, McRoberts, & Kändler, 2017). However, it is established that tree species characteristics, mostly canopy architecture, tree size, density, and age-related differences, create a pattern of gaps that vary through space and time, forming a complex mosaic of forest structure, composition and light environments in many landscapes (Frazer, Trofymow, & Lertzman, 2000; Trichon, Walter, & Laumonier, 1998; Lertzman, Sutherland, Inselberg, & Saunders, 1996). Subsequently, the precision of indirect LAI estimations is highly affected by such heterogeneous forest conditions and might render unreliable LAI predictions when used as an input variable in process-based models.

Despite the multitude of benefits (including rapidness, inexpensive, readily available data) derived from hemispherical photographs coupled with useful information on gap fractions which make it possible to estimate light regimes, leaf area index and leaf angle distribution,

obstacles emanating from image acquisition (field data collection) and software processing have pronounced effects on the accuracy of LAI estimations (Jonckheere et al., 2004).

Hemispherical photography has been used in a study implemented in the Swedish National Forest Inventory to estimate LAI. However, the magnitude of LAI precision has been barely investigated in such a changing vegetation biome of Sweden. In addition, basal area is a core variable in forest management and has widely been used for predicting individual tree or stand growth and yield, making optimal silvicultural decisions and for stand harvest planning. However, the linkage between indirect estimates of photo variables and basal area has been less explored in Swedish forest systems. Therefore, this present study sought to investigate this knowledge gap from climatic and stand variables in an attempt to provide reliable information on assessing the photosynthetic capacity of forested landscapes and increase the sensitivity of growth projection models to climate change.

The specific objectives were to:

a. Determine the variability of LAI or PAI (effective leaf area index) in varying forest types (dominant species) across northern and southern forest zones of Sweden, and

b. Explore the sensitiveness of effective leaf area index (LAIe) to different stand and site characteristics to ascertain whether stand attributes, radiation sums and PAI can improve basal area estimations across latitudinal gradients.

1.1 Research Questions

The study aims to address the following relevant questions:

a. How well could indirect estimates of leaf area index be used as a proxy for basal area estimation for Norway spruce, Scots pine and mixed forests?

b. Will species specific LAI functions improve basal area estimates compared to general PAI functions?

Could some of the variation between the indirect estimates and measured basal area be explained by variation in site conditions, climatic factors, forest structure (stem density, age and species composition)?

The study was organized in two sections. First, leaf and plant area indices were estimated from the sampled hemispherical photos and secondly, modelling of stand basal area from the estimated LAI and PAI, forest structure and climatic attributes.

2. Materials and Methods

2.1 Latitudinal gradient and forest cover description of Sweden.

The landscape of Sweden is characterized by a north-south gradient (the latitudinal range is from 55 °N to 69 °N), representing boreal to temperate vegetation zones (**Fig. 1**). Additionally, there is a pronounced variation in climate and soil conditions which are more favorable for tree growth in the south. Eight vegetation zones can be distinguished in Sweden; the boreal zone and its sub-zones cover the majority of the land area and are dominated by coniferous forests whereas, in the south, there is a small zone of mainly deciduous forests: the nemoral zone.

Forest land area is estimated to be 28.4 million hectares, upon which 22.7 million hectares are designated as productive forests (with growth more than 1 $m^3ha^{-1}year^{-1}$ of over-bark stem volume above stump) and 0.7 million hectares of productive forests within protected areas (Lundström and Wikberg, 2017). The dominant forest type is Scots pine forests which cover 39% of the Country's productive forest area. Other important forest types are Norway spruce forest (27%), mixed forest (22%) and deciduous forest (7%). The rest is composed of *Pinus contorta* (2%) and bare land (3%) (Lundström and Wikberg, 2017). Stands are classified into maturity stages based on normal management techniques; thinning stage forest and final felling forest represent the most-dominant maturity classes with 38 % and 33 % of productive forest area, respectively. On the other hand, young forest (including pre-commercial felling stage forest) and bare forest land contribute to 29 % of the productive forest area (Lundström and Wikberg, 2017).

Productivity (the growth potential of a site) is highest in the southernmost part of Sweden (11.0 $m^3ha^{-1}year^{-1}$) and then, decreases considerably in the northern and northwestern directions. However, the average site productivity for the entire country is 5.3 $m^3ha^{-1}year^{-1}$ per year (Lundström and Wikberg, 2017).

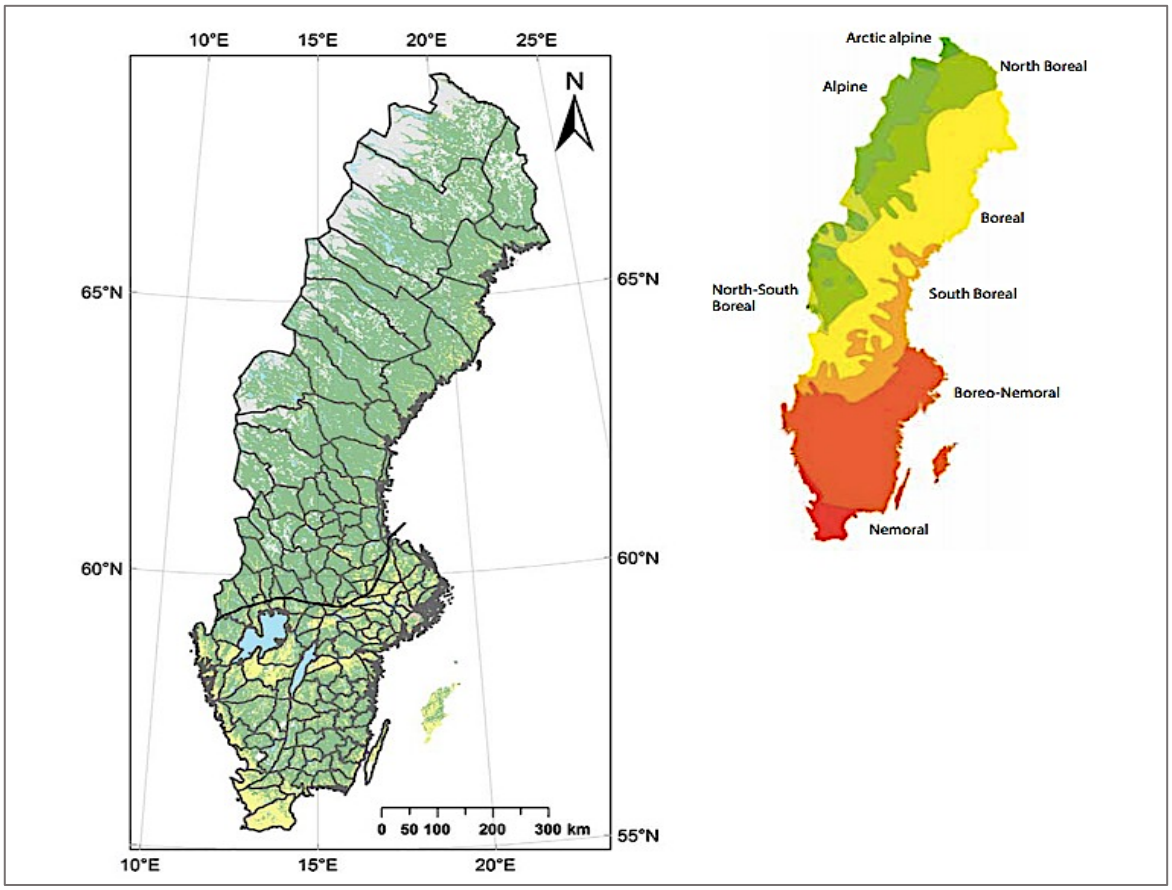

Fig. 1. Latitudinal gradient **(left)** and vegetation zones **(right)** of Sweden. Colors in lat-map indicate habitat types with forests in green, open habitats in yellow, freshwater in blue, urban areas in pink and mountains in grey [Source: adapted from Gentsch (2017, unpublished); https://www.skogsstyrelsen.se]

2.2 National forest inventory design and measurement of tree and stand attributes

The Swedish NFI (**Fig. 2**) is characterized by a systematic grid (with random starting point) of square and rectangular cluster plot designs (Axelsson et al., 2010). Presently, the total sample plots consist of 2500 temporary and 4500 permanent tracts. Each tract comprises 4 – 12 plots, with a varying side-length of 300 m and 800 m and are adapted to prevailing local conditions at different parts of the country, for example, the denser spacing in the south than in the north (Lundström and Wikberg, 2017). One-fifth of the whole sample is measured each year. About 12000 sample plots are used to inventory tree, stand and site attributes and conditions based on FAO (1997) definition of forests (*"Land with, or the potential of a forest with at least 10% crown cover and minimum height of trees of 5 m and a minimum area of 0.5 ha"*). Variable plot sizes (of radii 7-m and 10-m) and types (main, sub-plot, enlarged) are used to sample trees for measurement (Lundström and Wikberg, 2017). Diameter is measured for all

trees having a diameter at breast height (dbh) ≥10 cm on the main plot (7-m radius for temporary plots and 10-m radius for permanent plots), and for trees with dbh of 4–10 cm on a 3.5 m radius subplot (Lundström and Wikberg, 2017). Additionally, height, age, damages and other variables are measured on the sample trees. Saplings with a height range from 30 cm and up to dbh of 4 cm are counted in height interval classes at two 1-m radius plots (Lundström and Wikberg, 2017). The stand is characterized by defined height-interval-classes (species mixture, number of stems, etc.) for an enlarged 20-m radius plot. Other key variables such as basal area, volume, growth, biomass per tree compartment (stumps, branches, needles, and stemwood) and climatic parameters are derived from the NFI data (Lundström and Wikberg, 2017).

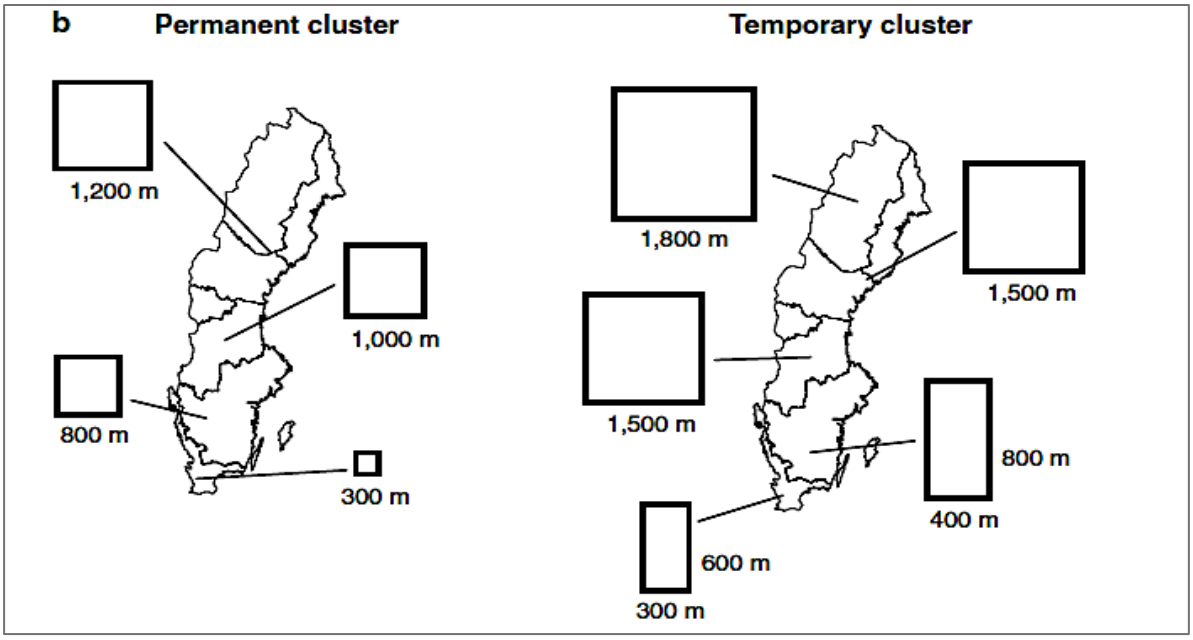

Fig 2. Regional division and size variation for permanent and temporary clusters in Sweden**.** [Source: Axelsson et al., (2010) cited in (Lawrence, McRoberts, Tomppo, Gschwantner, & Gabler, 2010)].

2.3. The sampling of hemispherical photographs, characterization, and processing

Study 1: Leaf area index estimation

Fish-eye photos (with image size of 4000 x 6000) were sampled from the plot centres of NFI plots from May to September in both 2016 and 2017 using Nikon D5300 camera. Sample plots in forest regenerations, with mean top height below 4 m were excluded from the final dataset.

Photos were categorized into three main groups, '**High- and Low- standards** and **Discarded** on the basis of pros and cons of image acquisition (Table 1) to test for practical efficiency. Images were visually assessed using canopy conditions, sky conditions and camera aperture exposition (Chianucci & Cutini, 2012). Nonetheless, photos in which there was a larger field of view, strong diffuse light and other undesirable parts (such as image covering only a single tree) beyond pre-processing corrections, were discarded. Examples of photo-grades are illustrated in **Fig. 3a** and **3b** below.

Analysis of photos to estimate LAI and other canopy attributes was done using the CAN-EYE software (version 6.4.91) developed at the EMMAH laboratory (Mediterranean environment and agro-hydro system modeling) in the French National Institute of Agricultural Research.

Table 1. Grading criteria for hemispherical photographs acquired in NFI plots

Photo-type	Threshold grading	Reasons	Reference
High standard	When more than 80% of the primary reasons exist in a photo.	Uniform overcast sky; fully developed canopy; camera lens oriented towards the magnetic north; a longer distance between canopy and camera lens; image exposition (aperture threshold).	(Liu & Pattey, 2010); (Leblanc, Chen, Fernandes, Deering, & Conley, 2005); (Welles & Norman, 1991); (Zhang, Chen, & Miller, 2005); (Macfarlane et al., 2007).
Low standard	About 40% of the primary reasons occur in a photo.		

In CAN-EYE, (Bonhomme, 1972) and (Weiss et al., 2004) recommended a zenith angle of 57.5° inclined from the vertical to measure canopy gap fraction, given that beyond this inclination angle, the extinction coefficient is largely independent of the foliage angle distribution (**Fig. 3d**).

In the preprocessing stages, initial calibration was done to characterize the fish-eye lens and camera type. Then, photos were parameterized in the upward color digital hemispherical photos (DHP) using an optical center, projection function as well as angular projection. CAN-EYE performs much better with polar projections where angular distances (in degrees) in the object's region are proportional to radial distances in pixels on the image plane (Hughes, Denny, Jones, & Glavin, 2010). In that, a first-degree polynomial function with a coefficient of 0.05538 corresponding to image size of 4000 x 6000 was used to derive the required polar

projection. This was done to standardize all sampled photos with the same calibration extent and to avoid the inconsistencies in photos with larger field of view. A default clumping parameter index of 8 was used throughout the photo analysis. However, undesirable parts of the photos were masked-out, images were sharpened to enhance the contrast between sky and canopy in class pre-selection by thresholding excess blue and green indices (**Fig. 3c**).

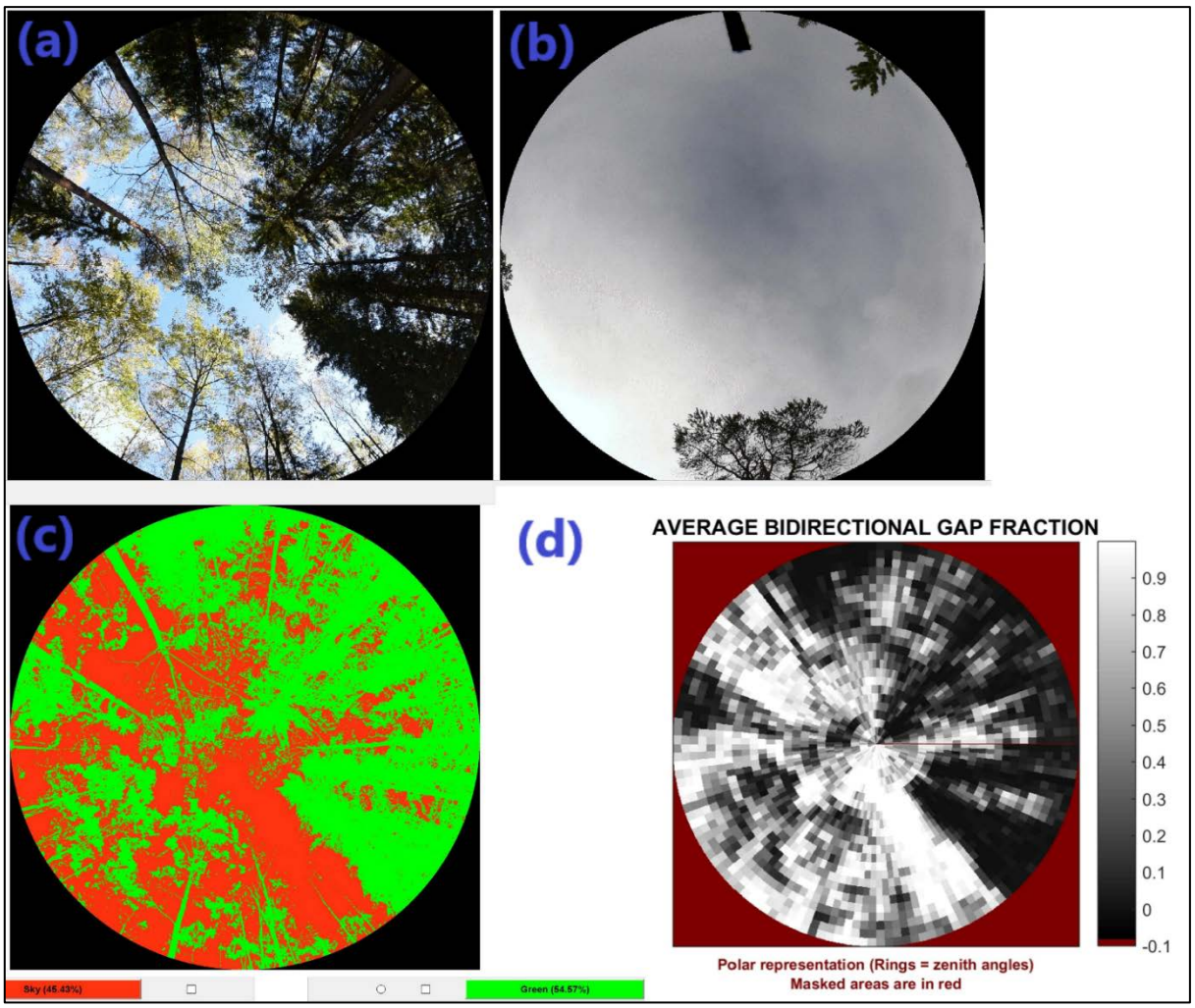

Fig. 3. Photo quality defined by grades of: **(a)** high standard and **(b)** low standard owing to non-uniform over sky conditions and irregular exposition; **(c)** class pre-selection by thresholding sky (red) and vegetation (green); **(d)** analysis of gaps using rings corresponding to the zenithal directions (darker pixels are vegetation components and brighter pixels represent sky).

Canopy structure characteristics such as plant area index was extracted from the fourth ring zenithal directions and used for further analysis. The CAN-EYE software estimates LAI (effective) as plant area index, an indirect estimate that comprises plant features such as stems,

branches and plant reproductive parts (Bouriaud, Soudani, & Bréda, 2003). A total of 449 sampled photos across northern and southern gradients were then used for the final analysis.

Study 2: Basal area estimation and modelling

This section involved developing models for estimating stand basal area from the estimated leaf area index in study 1 above, climatic variables and forest structure attributes.

2.4 Acquisition of climate predictors for canopy attributes modelling

Monthly photosynthetic active radiation sum (PAR) and global radiation sums, precipitation sum and mean monthly temperatures (minimum, maximum and mean) were obtained from the Japanese 55-year Reanalysis (JRA – 55) (Data acquisition by SMHI). The PAR variable is defined as radiations within 400 – 700 nm wavebands that plants can use to chemically synthesize their food and for growth (Harada et al., 2016). JRA – 55 Reanalysis is based on improved analysis methods and offers the best horizontal resolution of approximately 55 km. Additionally, JRA – 55 provides PAR data covering the entire of Sweden for the time period 1960 – 2016. The monthly PAR sums were multiplied by temperature and vapour pressure deficit modifiers to estimate the monthly absorbed PAR (APAR). Vapour pressure deficit was estimated (**Equation 2**) from the monthly maximum and minimum temperatures as half the difference between the saturated vapour pressure at maximum and minimum temperatures. Average vapour pressure deficit was logically related to temperature differences because water is lost from the air at the minimum temperature as dew (Mason, Holmström, & Nilsson, 2018). Soil vapour pressure was computed using the Tetens formula (**Equation 1**) as specified by (Monteith & Unsworth, 2008) for temperatures above 0 ^{0}C;

$$P = 0.61078 \exp\left(\frac{17.27\ T}{T+273.3}\right) \quad \textbf{(1)}$$

Where temperature T is in degrees Celsius (^{0}C) and saturated vapour pressure P in kilopascals (kPa). Therefore, vapour pressure deficit was estimated as:

$$VPD = 0.5 * [(0.61078 \exp\left(\frac{17.27\ Tmax}{Tmax+273.3}\right) - \left(0.61078 \exp\left(\frac{17.27\ Tmin}{Tmin+273.3}\right)\right] \quad \textbf{(2)}$$

Where in **Equation (2)**, VPD is the vapour pressure deficit in kilopascals (kPa), Tmax and Tmin are monthly maximum and minimum temperatures in degrees Celsius (^{0}C) respectively.

A VPD modifier on radiation use (PARFvpd) which is identical to the current version of the 3-PG model was represented as:

$$\text{PARFvpd} = \text{PAR}\,(e^{-0.05VPD}) \quad \textbf{(3)}$$

Where in **Equation (3)**, PAR is monthly radiation sums, e is the base of the natural logarithm.

The effect of temperature on radiation use (PAR * Ftemp) was based on the minimum, optimum and maximum temperatures for photosynthesis as:

$$\text{Ftemp} = \left(\frac{\text{Tec}-\text{Tmin}}{\text{Topt}-\text{Tmin}}\right)\left(\frac{\text{Tmax}-\text{Tec}}{\text{Tmax}-\text{Topt}}\right)^{\wedge(\text{Tmax}-\text{Topt})/(\text{Topt}-\text{Tmin})} \quad \textbf{(4)}$$

Where in **Equation (4)**, Ftemp = 0 if Tec ≤ Tmin or Tmax ≤ Tec, Ftemp is temperature modifier and Tmin, Topt, and Tmax represent the minimum, optimum and maximum air temperatures for net photosynthetic production in degrees Celsius. Tec is the mean temperature for each month. However, temperature modifier on radiation use differed among species and hence, the minimum, optimum, and maximum temperatures for photosynthesis were assumed to be -2 ^{0}, 15 ^{0} and 25 ^{0}, respectively for Scots pine-dominated stands (Kolari, Lappalainen, Hänninen, & Hari, 2007). In Norway spruce, -3 ^{0}, 20 ^{0} and 43^0 were also assumed as the minimum, optimum and maximum temperatures for photosynthesis, respectively (Bergh et al., 2003). In broad-leaved forests, the minimum, optimum and maximum temperature values were 8.5 ^{0}, 24.5 ^{0} and 36 ^{0}, respectively (Potithep & Yasuoka, 2011). Relationship between temperature modifiers and monthly mean temperatures is visualized in **Fig. 4** for all sample plots for the year 2015. At monthly mean temperatures of 0 ^{o}C, there is the likelihood of 20 % utilization of absorbed PAR in conifers whereas, broadleaves require temperatures above 10 ^{o}C to achieve similar utilization efficiency.

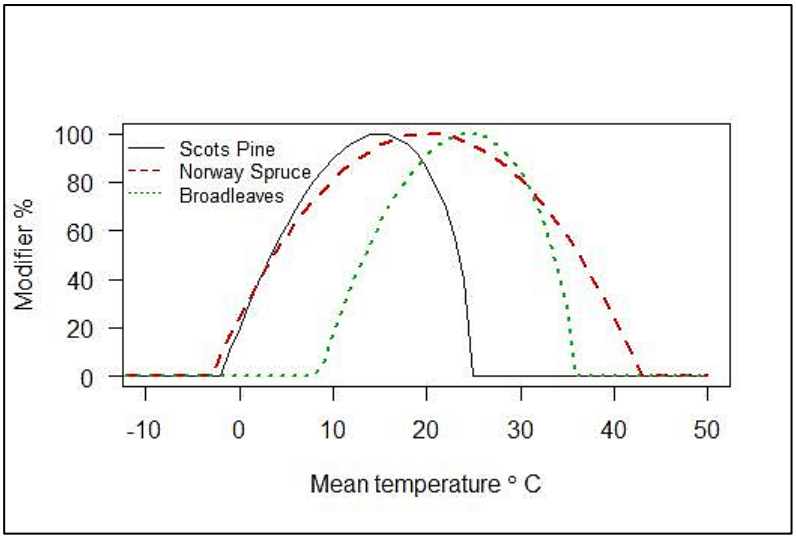

Fig. 4. Relationships among temperature modifiers of Norway spruce, Scots pine and Birch and the mean temperatures for all sample plots in latitudinal gradient of Sweden across a randomly selected year of 2015. Modifiers are scaled between 0 and 100 %, characterizing a decrease and an increase in the efficiency of radiation conversion, respectively.

Monthly PAR and PAR-modified values from January to December were aggregated to annual sums and then, the individual annual PAR sums averaged across the 10-year period (2005 – 2015). Therefore, PAR sums were accumulated for unmodified radiation, PAR modified only by temperature and PAR modified by both temperature and vapour pressure deficit. These different PAR sums were tested as covariates in all PAI modelling by dominant species.

Evapotranspiration was computed using the Penman-Monteith equation with inputs of monthly mean temperature, wind speed, relative humidity and solar radiation (read in depth information in (Landsberg & Sands, 2011). However, the effect of water on canopy leaf area development was investigated with both humidity (excess water) and drought (deficient-water) in the summer months (May, June, July, and August) of the growing season.

Soil fertility was characterized by the field-layer-vegetation type scaled in the interval (index) of -5 (nutrient-deficient) to +4 (nutrient-rich) as proposed by Elfving (2010, unpublished) in developing soil fertility modifiers for the Heureka system. The scaling described vegetation ranges from tall herbs without dwarf-shrubs through to narrow-leafed grasses, bilberries and lichens (Table 2).

Table 2. Site productivity characterised by vegetation types

Vegetation description	Swedish	NFI[b] code	Vegetation index[a]
Tall herbs without shrubs	H-ört u ris	1	4
High herbs with bilberries	H-ört m blå	2	2.5
High herbs with cowberry	H-ört m ling	3	2
Low herbs without shrubs	L-ört u ris	4	3
Low herb with bilberries	L-ört m blå	5	2.5
Low herb with cowberry	L-ört m ling	6	2
Soil without field layer	Utan fs	7	3
Broad-leaved grasses	Breda gräs	8	2.5
Thin-leaved grasses	Smala gräs	9	1.5
Sedge-horsetail	Högstarr	10	-3
Sedge-horsetail	Lågstarr	11	-3
Sedge-horsetail	Fräken	12	1
Bilberries	Blåbär	13	0
Cowberry	Lingon	14	-0.5
Crowberry-heather	Kråkb/ljung	15	-3
Dwarf shrub	Fattigris	16	-5
Lichen-rich	Lavrik	17	-0.5
Lichens	Lav	18	-1

Note: [a] vegetation indices created by Elfving (2010, unpublished); [b] represents vegetation code used in the Swedish NFI.

2.5 Model development and statistical data analysis

To model canopy structure-climatic-topographic-land-uses, Pearson moment of product correlation (**r**) was used to visualize the relationships among the numeric predictors for each species model (**Fig. 5**). Variable pairs with '**r'** greater than 0.6 were considered highly-correlated hence, excluded from the initial model building. This approach was considered useful in an attempt to avoid the problems of multicollinearity and over-fitting when combining predictors. In addition, the presence of multicollinearity was assessed using variance inflation

measure employed in Farrar-Glauber test (mctest package in R) (Imdadullah, Aslam, & Altaf, 2016). These two approaches for testing multicollinearity demonstrated similar results.

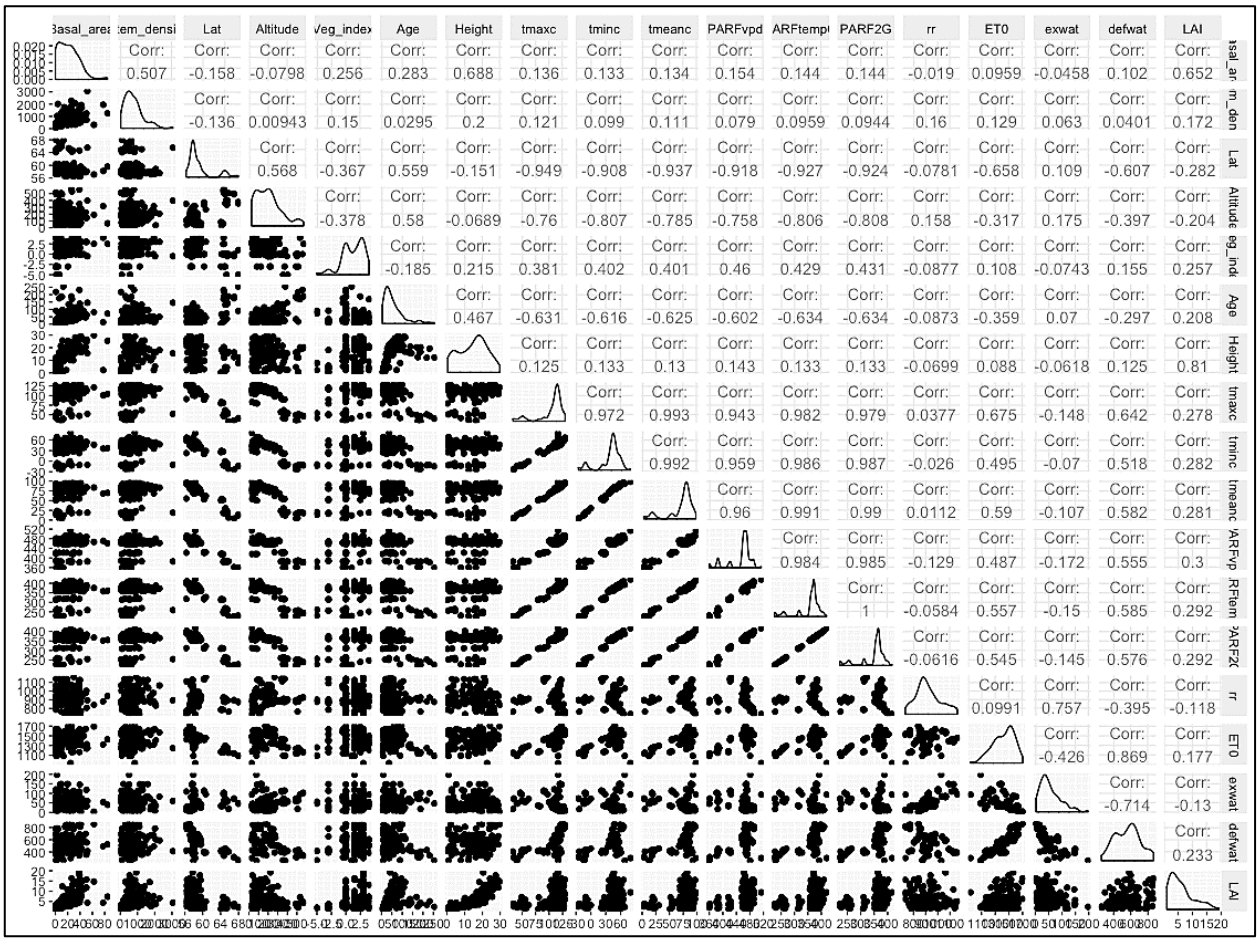

Fig. 5. Visualization of multicollinearity among model predictors for Norway spruce. Threshold for characterization of multicollinearity is 60 % (**r > 0.60**).

Normality testing and variance homogeneity were done using Shapiro-Wilk test (Royston, 1995) and Fligner Killeen's test employed in R statistical environment (R Core Team, 2017), respectively. Results shown non-normality and heterogeneous variances of canopy attributes, stand and climate predictors ($p<0.05$).

Prior to model building, the inventory data for each sample plot was used for calculations of sample plot data of basal area (m^2 ha^{-1}) and stem density (stems ha^{-1}). All calipered trees at 1.3 m dbh were converted to basal area (**Equation 5**) and stem density and aggregated to per hectare units at the plot level using respective sample plot sizes (**Equation 6**).

$$\mathrm{BA} = \frac{\prod D^2}{4} \qquad (\mathbf{5})$$

$$\mathrm{EF} = \frac{10000}{plot\ area} \qquad (\mathbf{6})$$

Where **in Equations (5 and 6),** BA and EF are the estimated basal area and expansion factor to convert estimates to per hectare units, respectively, D is the calipered tree diameter (m) at 1.3 m at breast height.

Other variables such as mean top-height (OH), land-use (forest, pasture, high mountains, mire and bare rock) and dominant species were compiled for each plot. Thus, stands having more than 80 % of density of a single species were classified as mono-species forests and below this threshold, stands were classified as mixed-species forests. Subsequently, mono Scots pine, mono Norway spruce, mixed conifers and mixed broadleaves (comprising Birch and other broad-leaved species) classes were categorized. Furthermore, significant conversion models (**Equations 7 and 8**) for Norway spruce (R^2 = 0.78, $p < 0.01$) and Scots pine (R^2 = 0.59, $p < 0.01$) were used to estimate LAI from PAI, respectively (Goude, 2018, unpublished). However, lack of existing models for mixed coniferous forests, birch and other broadleaves resulted in the use of PAI for species specific modelling;

$$\mathrm{LAI} = \exp^{0.673(\mathrm{PAI}) + 0.063(\mathrm{OH}) + 0.021} \qquad \mathbf{(7)}$$

$$\mathrm{LAI} = 2.472\ (\mathrm{PAI}) + 1.184 \qquad \mathbf{(8)}$$

Where **in Equations (7 and 8)**, LAI is the estimated leaf area index and PAI is the plant area index computed from the fourth ring of CAN-EYE, OH is the mean top-height.

Species specific models were built using a stepwise regression approach from the base packages of *caret* and *MASS* in R (R Core Team, 2017). This approach was carried out iteratively to select variables that enhances the best performance of the models, thus a model that lowers prediction error (Tibshirani, James, Witten, & Hastie, 2013). The "lmStepAIC" method allows an option for direction which involves both 'forward and backward' selection of predictive variables (Tibshirani et al., 2013). First, the model works with no predictors, then contributive climate, stand and site indicators were sequentially added (forward selection). Afterwards, variables that do not improve the model fit are systematically removed (backward selection).

A 10-fold cross-validation was created as a training control parameter and set to a reproducibility of '123' to estimate the average prediction error (residual mean square error) of

the best model-fit. Finally, model predictors were reported for their estimates (coefficient and direction), standard error, the test-statistics (t-value) and the level of significance (p-value). Residual diagnosis for each model was investigated by examining the plots of normality and variance homogeneity of fitted values of dependent (basal area) and independent (climate and stand) variables.

Table 3. Summary of key stand and site characteristics for species specific models. Values represent range (min – max) of the variable.

Variable	Norway spruce (mono)[b]	Scots pine (mono)[b]	Mixed conifers	Broadleaves
Climate				
Latitude range (^{o}N)	56 – 68	57 - 68	56 – 68	56 - 67
Altitude (m, a.s.l)	27 – 570	11 – 476	5 – 580	2 – 765
[a]Minimum temperature (^{0}C)	-25 – 80	-28 – 81	-27 – 81	-39 – 99
[a]Maximum temperature (^{0}C)	33 – 130	31 - 129	32 - 130	18 – 129
[c]Precipitation (mm y^{-1})	733 – 1160	684 – 1160	684 – 1160	667 – 1128
[a]Modified PAR (MJ m^2 y^{-1})	222 – 416	230 – 434	235 – 434	32.33 – 226
Stand				
Basal area (m^2 ha^{-1})	1.4 – 51.9	5.1 – 43.6	4.0 – 34.0	4.0 – 48.5
[b]LAI / PAI (m^2 m^{-2})	1.1 – 19.2	1.2 – 3.6	0.01 – 2.0	0.1 – 2.0
Stand density (trees ha^{-1})	32 - 3053	127 - 2144	32 - 2899	95 - 1965
Mean top-height (m)	4.0 – 29.0	4.6 – 26.0	4.0 – 25.8	4.2 – 27
Stand age (years)	8 – 255	20 – 230	9 – 230	8 – 146
Sample plots (n)	126	123	142	58

[a] Estimates are averages of annual sums for a 10 – year period (2006 -2015 for NFI 2016 and 2007-2016 for NFI 2017).

[b] Values represent LAI for only Norway spruce and Scots pine; others are PAI estimates.

[c] Range values for precipitation are averages of 10-year annual sums for summer months only (June to August).

3. Results

3.1 Estimation of leaf and plant area indices

Generally, patterns of relationships between measured basal area and indirect estimate of leaf area index showed increasing trends for all forest types (Fig. 6).

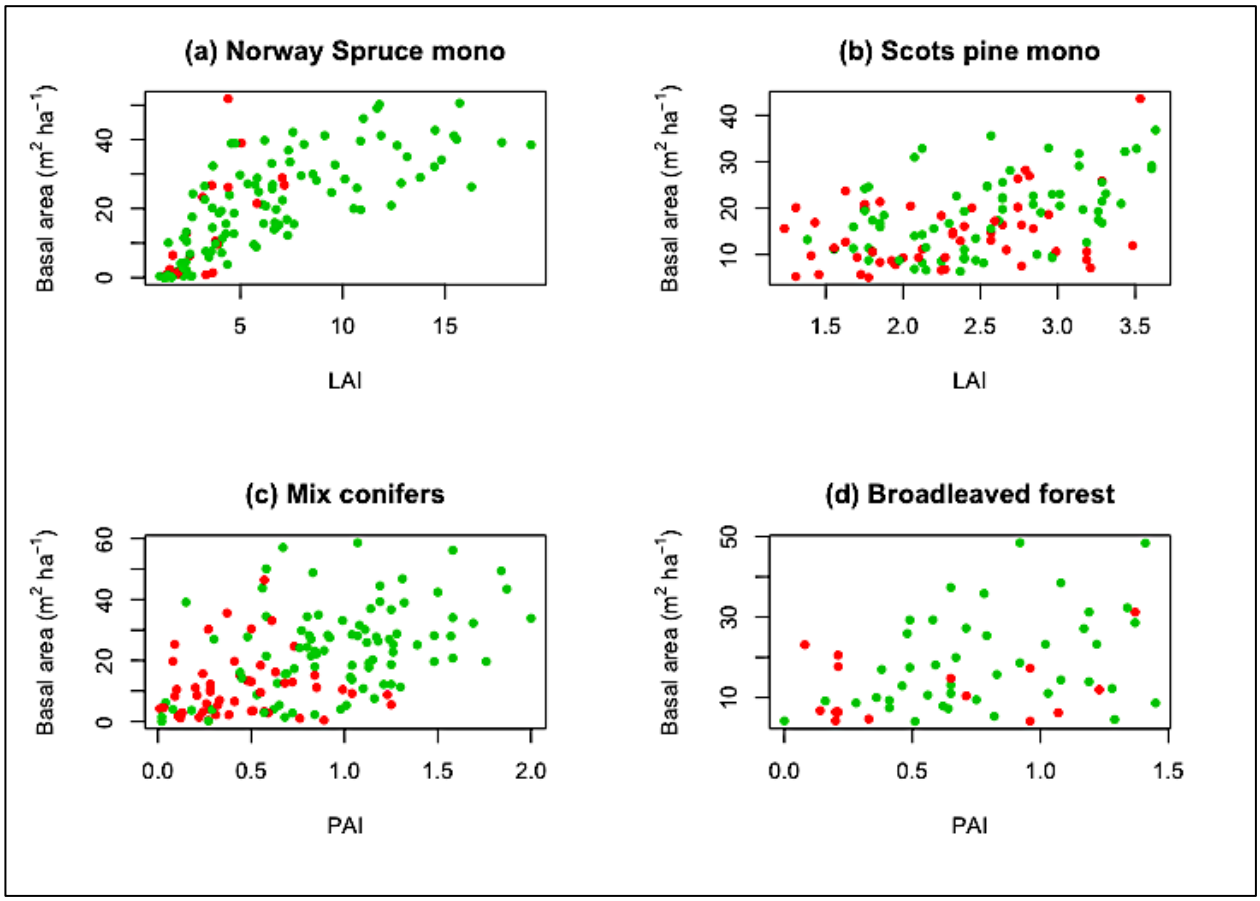

Fig. 6. Scatter plots delineating patterns of basal area and leaf area index estimations for different forest types. Red and green-filled points are values from northern and southern Sweden respectively.

3.2 Estimation of basal area from stand and site variables.

Basal area estimation with indirect estimates of leaf area was significant ($p < 0.001$) for all species (Table 4). Explained variations with only LAI functions were significantly higher for Norway spruce (54 %) and Scots pine (40 %), than in mixed forests using general PAI functions.

Table 4. Analysis of variance of basal area relationships with leaf and plant area index

Source of variation	Norway spruce	Scots pine	Mixed coniferous	Mixed broadleaves
LAI / PAI (ssq)	13924	1528.9	7110.7	1025.1
Residuals (ssq)	5568	6237.2	21300.8	6194.1
Df	(1,119)	(1,121)	(1,140)	(1, 56)
F-value	297.6	29.66	46.74	9.27
p-value	< 2.2e-16 ***	2.747e-07 ***	2.308e-10 ***	0.00355 **
R^2 adj.	54 %	40 %	24 %	13 %

Note: ssq is sum squares, Df is degree of freedom. Significant anova test for all species at $p < 0.001$.

Including stand and site characteristics also significantly improved the basal area estimation for each tree species or forest type (Table 5). Species specific models with LAI functions significantly increased the basal area estimation compared to models with PAI functions. Stem density improved the prediction for all species categories, while mean top height, age and APAR added small, but significant contribution to the models.

The share of variation explained by all predictors varied considerably for each tree species, thus ranging from 77 % and 71 % in monocultures of Norway spruce and Scots pine respectively, mixed coniferous and broad-leaved forests each accounted for 60 % of the variation. Furthermore, the residual standard error (m^2 ha^{-1}) was highest in 8.966 in mixed conifers, broad-leaves (7.141), Norway spruce mono (6.840) and lowest in Scots pine mono (4.310).

Residual diagnosis showed that models with LAI functions did not show any systematic deviation evaluated on basal area, age or stem density for the monocultures of Norway spruce and Scots pine compared to broad-leaved models with PAI functions (**Fig. 7**). Residuals of mixed coniferous forest – models (with PAI functions) were also adapted to predicted basal area and stem density, though the model overestimates in older stands with age above 150 years.

Table 5. Functions for basal area estimation in different forest types.

Model predictors	Coefficient	Std. Error	t-value	P-value
Norway spruce (mono)				
Intercept	-19.517	5.629	-3.467	0.00073 ***
LAI	1.088	0.26683	4.078	8.23e-05 ***
Stem density	0.00959	0.00121	7.906	1.51e-12 ***
Age	0.04091	0.01797	2.277	0.02460 *
Mean top-height	0.69605	0.16784	4.147	6.35e-05 ***
Land-use (prod. forest)	4.079	4.486	0.909	0.049 *
RMSE	6.840			
R^2 adj.	77 %			
F (6, 119)	71.90			<2.2e-16
Scots pine (mono)				
Intercept	-19.845	2.450	-8.099	6.22e-13 ***
LAI	2.080	0.70011	2.971	0.00361 **
Stem density (trees ha^{-1})	0.01321	0.00118	11.192	< 2e-16 ***
Mean top-height (m)	1.413	0.12421	11.373	< 2e-16 ***
Land-use (pasture)	-8.195	3.595	-2.280	0.024475 *
Land-use (prod. forest)	-4.674	1.582	-2.955	0.00379 **
Excess water (mm yr^{-1})	0.03190	0.00926	3.445	0.00079 ***
RMSE	4.310			
R^2 adj.	71 %			
F (6, 116)	50.34			< 2.2e-16
Mixed Conifers				
Intercept	-32.221	5.481	-5.878	3.01e-08 ***
PAI	5.795	2.031	2.853	0.005 **
Stem density (trees ha^{-1})	0.01490	0.00166	8.982	1.86e-15 ***
Stand age (years)	0.10051	0.01773	5.668	8.21e-08 ***
PARF2T (MJ m^{-2} yr^{-1})	0.08625	0.01599	5.393	2.95e-07 ***
RMSE	8.966			
R^2 adj.	60 %			
F (4, 137)	54.11			< 2.2e-16
Broadleaves				
Intercept	-9.198	3.261	-2.821	0.00672 **
PAI	5.262	2.554	2.060	0.04428 *
Stem density (trees ha^{-1})	0.00982	0.00294	3.332	0.00158 **
Mean top-height (m)	1.109	0.16370	6.780	1.02e-08 ***
Land-use (Pasture)	-8.065	3.322	-2.428	0.01861 *
RMSE	7.141			
R^2 adj.	60 %			
F (4, 53)	22.15			8.644e-11

Note: Dependent variable = Basal area (m^2 ha^{-1}). Independent variable: climate, stand and land-use characteristics. Predictors are significant at $p < 0.0001$ '***', $p < 0.001$ '**'and $p < 0.01$ '*' probability levels. RMSE is the residual standard error (m^2 ha^{-1}) for fitted models and F shows the test-value for overall model significance.

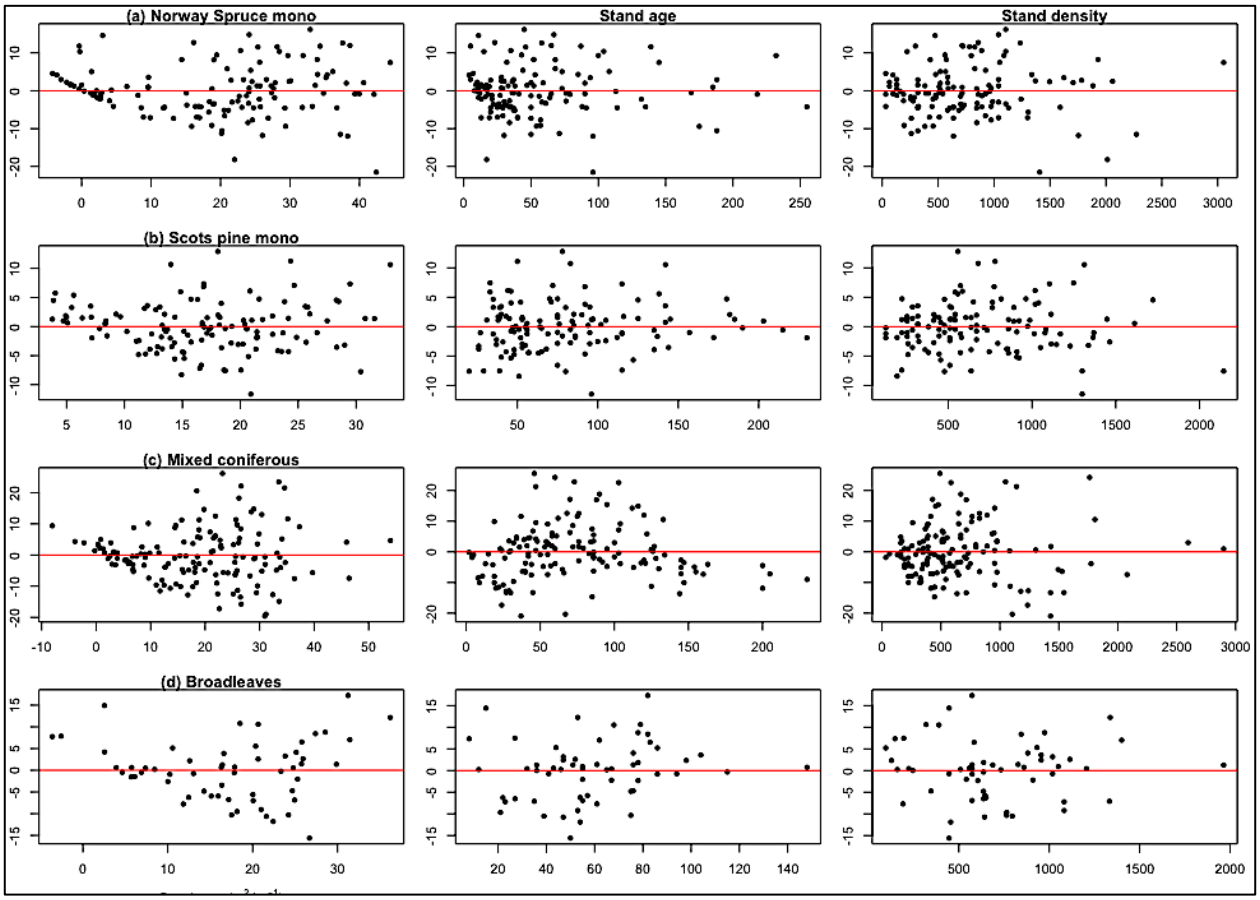

Fig. 7. Residual (m^2 ha^{-1}) diagnostic plots for fitted models plotted over left panel, predicted basal area (m^2 ha^{-1}), middle panel, stand age (years) and right panel, stem density (trees ha^{-1}) for **a)** Norway spruce mono **b)** Scots pine mono **c)** Mixed coniferous forest and **d)** Broad-leaved forests.

4. Discussion

4.1 Species specific models for prediction of stand basal area from site characteristics

In general, the models were well adapted to the data as residuals did not show any systematic deviations over predicted basal area, stand age and stem density for all tree species. Though, indirect leaf area estimation methods systematically underestimate the leaf area index of a forest type, the availability of conversion functions from PAI to LAI could guarantee improved estimates in tree growth and yield modelling. Using LAI functions in monocultures of Norway spruce and Scots pine explained much of the variations in the model than the general PAI functions used in modelling basal area estimation for mixed coniferous and broad-leaved forests. Residual standard errors of fitted models decreased considerably in species models with LAI functions compared to larger standard errors in models enhanced with general PAI values. The unexplained variations in the models could be attributed to improved planting materials and advanced silvicultural management techniques. However, future models should be designed to capture these effects.

The significance of PAI and LAI variables in the models illustrates the physiological roles exhibited by forest canopies on the basis of resources acquisition, efficiency of photosynthesis and the distribution of photosynthetic products to other tissues and organs of the plants (Binkley, Stape, & Ryan, 2004). Generally, tree crowns are described by the number and architectural characteristics of leaves (leaf area) and several studies have reported significant positive relationships with higher leaf area stand productivity (Binkley, Stape, & Ryan, 2004). Binkley, Campoe, Gspaltl, & Forrester (2013) reported that light interception is a function of the amount of leaves within the tree crowns, though this function is non-linear at higher leaf area values. Increase in leaf area index leads to higher sapwood formation in trees. Stem diameter (basal area) increases with increasing sapwood content (West 2013), hence significant in all models. However, this trend decreases with tree age as more non-conducting woody cells are produced, limiting the conductivity of water and subsequent decline in tree growth (West, 2014).

Incorporating stem density as covariate improved the relationship between indirect estimates of leaf area index and basal area estimation for all species. The density of a stand could describe the canopy structure and provide useful links towards radiation interception.

Stem density influences water and nutrient availability through competition for growth resources (Landsberg & Sands, 2011). Stem density also affect canopy development over a rotation. Closely spaced (high densities) trees in even-aged monocultures have less canopy gaps and early canopy closure. This fosters higher production due to strong interception of light (Cannel, 1989).

Stand age also had significant contribution in basal area estimation for Norway spruce and mixed conifers. Models characterizing stand productivity from relative age have shown that aboveground net primary production decreases as forest stand ages (Landsberg & Waring, 1997). Yoder et al. (1994) attributed this to the sensitivity of stomata cells to atmospheric vapor pressure deficit. As tree height increases with age, the greater the gravitational force resisting the upward movement of water and this causes water stress in leaves (West, 2014). Other studies by Ryan & Yoder (1997) reported that hydraulic conductivity decreases as trees get older limiting the flow of water due to damaged xylem vessels. Mencuccini & Grace (1996) found a significant linear relationship between hydraulic conductance and net primary production in Scots pine stands with a 50-year age difference, lower values of net production and hydraulic conductance were recorded in older stands and highest values associated with younger stands. Subsequently, lower stem conductance induces lower stomatal conductance, resulting in reduced photosynthesis and less carbon is available to sustain the already established leaf area.

Tree height was also substantial to the final models. Height represent an indicator variable for characterizing site potential (site index) and taller trees have larger stem wood which provides mechanical strength and serve as conducting routes for water transportation to roots (West, 2014). Ecologically, tall tree height plays supportive role in holding leaves high up in the air for the tree to receive much sunlight, supports the total tree weight and provides strong resistance to stresses of wind (West, 2014; King et al., 2009). so, the larger must be the stem diameter to hold it upright. Hence, the subsequent increase in tree basal area with increasing height.

It was also observed that including the site specific absorbed radiation increased the basal area prediction in mixed coniferous forests. Studies by Mason et al. (2018) to predict site index for Scots pine using physiological and mensurational variables revealed significant contributions from radiation-use efficiency and field vegetation. The efficiency of conversion of light into chemical energy is modified by the effects of temperature, atmospheric VPD, soil

drought, site nutrition and stand age (Landsberg & Waring, 1997). Generally, it was observed that values of PAR modified by temperature and VPD were lower in northern Sweden than in the southern part. This effect might be partially attributed to the longer growing season in southern Sweden (Bergh, Linder, & Bergström, 2005).

Water availability was significant for model estimation in monocultures of Scots pine, though it contributed marginally to the basal area estimate. Water availability triggers aboveground allocation of photosynthates than belowground. Several studies have also confirmed the effects of water shortage on efficiency of radiation conversion and partitioning of photosynthates in below and aboveground organs of plants (Waring, Landsberg, & Linder, 2016; Landsberg & Waring, 1997). Water balance doubles as indicator for assessing forest growth potential and improves the accuracy of models for tree growth prediction under varying climatic conditions. Boosma & Hunter (1990) confirmed that water deficits reduce stem growth and by restricting the development of leaf area, photosynthesis and stomatal conductance. In northern Sweden, Bergh et al. (2005) found out that water availability in summer months did not reduce the production capacity of Norway spruce, an effect attributed to higher levels of precipitation greater than evaporation. In addition, it was also observed that ground water recharge was complemented by the heavy snow melt prior to the start of growing season. On the other hand, opposite findings were observed in southern Sweden by (Bergh et al., 2005) where limited water decreased attainable volume production in Norway spruce.

This study has shown that using indirect leaf area estimates and other stand and climate variables have the potential to be used as independent variables for estimating basal area for different tree species in boreal forests of Sweden. However, suggestions for model improvements are highlighted below:

Firstly, due to the lack of conversion models from PAI to LAI, estimates of PAI were used for modelling basal area relationships in mixed conifers and broad-leaved forests. However, given the relevance of LAI in the use of physiological processes to estimate the photosynthetic capacity of a stand, converted PAI values would offer greater potentials in estimating stand basal area with higher precision.

Secondly, climate data were extracted from the Japanese 55-year Reanalysis (JRA – 55) which uses a 55 x 55 km grid (Harada et al., 2016) to provide monthly-time step data for the entire Sweden since 1960. But with recent advances in resolutions of digital elevation models,

species specific models could also be tested with relief features such as slope, aspect, spectral and textural variables and their relationships with stand productivity in Sweden.

References

Baret, F., & Buis, S. (2008). Estimating Canopy Characteristics from Remote Sensing Observations: Review of Methods and Associated Problems. In Advances in Land Remote Sensing (pp. 173–201). Springer, Dordrecht. https://doi.org/10.1007/978-1-4020-6450-0_7

Barreiro, S., Schelhaas, M.-J., McRoberts, R. E., & Kändler, G. (2017). Forest Inventory-based Projection Systems for Wood and Biomass Availability. Springer.

Bergh, J., Linder, S., & Bergström, J. (2005). Potential production of Norway spruce in Sweden. Forest Ecology and Management, 204(1), 1–10. https://doi.org/10.1016/j.foreco.2004.07.075

Bergh, J., Linder, S., Lundmark, T., & Elfving, B. (1999). The effect of water and nutrient availability on the productivity of Norway spruce in northern and southern Sweden. Forest Ecology and Management, 119(1), 51–62. https://doi.org/10.1016/S0378-1127 (98)00509-X

Bergh, J., Nilsson, U., Kjartansson, B., & Karlsson, M. (2010). Impact of climate change on the productivity of silver birch, Norway spruce and Scots pine stands in Sweden and economic implications for timber production. Ecological Bulletins, (53), 185–196.

Binkley, D., Campoe, O. C., Gspaltl, M., & Forrester, D. I. (2013). Light absorption and use efficiency in forests: Why patterns differ for trees and stands. Forest Ecology and Management, 288, 5–13. https://doi.org/10.1016/j.foreco.2011.11.002

Binkley, D., Stape, J. L., & Ryan, M. G. (2004). Thinking about efficiency of resource use in forests. Forest Ecology and Management, 193(1), 5–16. https://doi.org/10.1016/j.foreco.2004.01.019

Bonan, G. B. (1993). Importance of leaf area index and forest type when estimating photosynthesis in boreal forests. Remote Sensing of Environment, 43(3), 303–314. https://doi.org/10.1016/0034-4257 (93)90072-6

Bonhomme, R. (1972). The interpretation and automatic measurement of hemispherical photographs to obtain sunlit foliage area and gap frequency. Israel J Agric Res, 22, 53–61.

Boosma, D. B., & Hunter, I. R. (1990). Effects of water, nutrients and their interactions on tree growth, and plantation forest management practices in Australasia: A review. Forest

Ecology and Management, 30(1), 455–476. https://doi.org/10.1016/0378-1127 (90)90154-4

Bouriaud, O., Soudani, K., & Bréda, N. (2003). Leaf area index from litter collection: impact of specific leaf area variability within a beech stand. Canadian Journal of Remote Sensing, 29(3), 371–380. https://doi.org/10.5589/m03-010

Bréda, N. J. J. (2003). Ground-based measurements of leaf area index: a review of methods, instruments and current controversies. Journal of Experimental Botany, 54(392), 2403–2417. https://doi.org/10.1093/jxb/erg263

Cannel, M. G. R. (1989). Physiological basis of wood production: A review. Scandinavian Journal of Forest Research, 4, 459 - 490

Chason, J. W., Baldocchi, D. D., & Huston, M. A. (1991). A comparison of direct and indirect methods for estimating forest canopy leaf area. Agricultural and Forest Meteorology, 57(1), 107–128. https://doi.org/10.1016/0168-1923 (91)90081-Z

Chen J. M., & Black T. A. (2006). Defining leaf area index for non-flat leaves. Plant, Cell & Environment, 15(4), 421–429. https://doi.org/10.1111/j.1365-3040.1992.tb00992.x

Chen, J. M., & Cihlar, J. (1995). Quantifying the effect of canopy architecture on optical measurements of leaf area index using two gap size analysis methods. IEEE Transactions on Geoscience and Remote Sensing, 33(3), 777–787. https://doi.org/10.1109/36.387593

Chen, Jing M., & Cihlar, J. (1996). Retrieving leaf area index of boreal conifer forests using Landsat TM images. Remote Sensing of Environment, 55(2), 153–162.

Chen Jing M., Rich Paul M., Gower Stith T., Norman John M., & Plummer Steven. (1997). Leaf area index of boreal forests: Theory, techniques, and measurements. Journal of Geophysical Research: Atmospheres, 102(D24), 29429–29443. https://doi.org/10.1029/97JD01107

Chianucci, F., & Cutini, A. (2012). Digital hemispherical photography for estimating forest canopy properties: current controversies and opportunities. IForest - Biogeosciences and Forestry, 5(6), 290–295. https://doi.org/10.3832/ifor0775-005

Cohen, W. B., Maiersperger, T. K., Gower, S. T., & Turner, D. P. (2003). An improved strategy for regression of biophysical variables and Landsat ETM+ data. Remote Sensing of Environment, 84(4), 561–571. https://doi.org/10.1016/S0034-4257 (02)00173-6

Epiphanio, J. N., & Huete, A. R. (1995). Dependence of NDVI and SAVI on sun/sensor geometry and its effect on fAPAR relationships in Alfalfa. Remote Sensing of Environment, 51(3), 351–360. https://doi.org/10.1016/0034-4257 (94)00110-9

Fassnacht, K. S., Gower, S. T., Norman, J. M., & McMurtric, R. E. (1994). A comparison of optical and direct methods for estimating foliage surface area index in forests. Agricultural and Forest Meteorology, 71(1), 183–207. https://doi.org/10.1016/0168-1923 (94)90107-4

Franklin, S. E., Lavigne, M. B., Deuling, M. J., Wulder, M. A., & Hunt Jr, E. R. (1997). Estimation of forest leaf area index using remote sensing and GIS data for modelling net primary production. International Journal of Remote Sensing, 18(16), 3459–3471.

Frazer, G. W., Trofymow, J. A., & Lertzman, K. P. (2000). Canopy openness and leaf area in chronosequences of coastal temperate rainforests. Canadian Journal of Forest Research, 30(2), 239–256. https://doi.org/10.1139/x99-201

Friedl, M. A., Schimel, D. S., Michaelsen, J., Davis, F. W., & Walker, H. (1994). Estimating grassland biomass and leaf area index using ground and satellite data. International Journal of Remote Sensing, 15(7), 1401–1420. https://doi.org/10.1080/01431169408954174

Gobron, N., Pinty, B., & Verstraete, M. M. (1997). Theoretical limits to the estimation of the leaf area index on the basis of visible and near-infrared remote sensing data. IEEE Transactions on Geoscience and Remote Sensing, 35(6), 1438–1445. https://doi.org/10.1109/36.649798

Gower, S. T., Kucharik, C. J., & Norman, J. M. (1999). Direct and Indirect Estimation of Leaf Area Index, fAPAR, and Net Primary Production of Terrestrial Ecosystems. Remote Sensing of Environment, 70(1), 29–51. https://doi.org/10.1016/S0034-4257 (99)00056-5

Harada, Y., Kamahori, H., Kobayashi, C., Endo, H., Kobayashi, S., Ota, Y., Takahashi, K. (2016). The JRA-55 Reanalysis: Representation of Atmospheric Circulation and Climate Variability. Journal of the Meteorological Society of Japan. Ser. II, 94(3), 269–302. https://doi.org/10.2151/jmsj.2016-015

Hardwick, S. R., Toumi, R., Pfeifer, M., Turner, E. C., Nilus, R., & Ewers, R. M. (2015). The relationship between leaf area index and microclimate in tropical forest and oil palm plantation: Forest disturbance drives changes in microclimate. Agricultural and Forest Meteorology, 201, 187–195. https://doi.org/10.1016/j.agrformet.2014.11.010

He, Y., Guo, X., & Wilmshurst, J. F. (2007). Comparison of different methods for measuring leaf area index in a mixed grassland. Canadian Journal of Plant Science, 87(4), 803–813. https://doi.org/10.4141/CJPS07024

Hughes, C., Denny, P., Jones, E., & Glavin, M. (2010). Accuracy of fish-eye lens models. Applied Optics, 49(17), 3338–3347. https://doi.org/10.1364/AO.49.003338

Hunt, T. E., Haile, F. J., Hoback, W. W., & Higley, L. G. (1999). Indirect Measurement of Insect Defoliation. Environmental Entomology, 28(6), 1136–1139. https://doi.org/10.1093/ee/28.6.1136

Imdadullah, M., Aslam, M., & Altaf, S. (2016). mctest: An R Package for Detection of Collinearity among Regressors. The R Journal, Online Published Paper, 3.

Johnson I. R., & Thornley J. H. M. (2006). Vegetative crop growth model incorporating leaf area expansion and senescence, and applied to grass. Plant, Cell & Environment, 6(9), 721–729. https://doi.org/10.1111/1365-3040.ep11588103_6_9

Jonckheere, I., Fleck, S., Nackaerts, K., Muys, B., Coppin, P., Weiss, M., & Baret, F. (2004). Review of methods for in situ leaf area index determination: Part I. Theories, sensors and hemispherical photography. Agricultural and Forest Meteorology, 121(1), 19–35. https://doi.org/10.1016/j.agrformet.2003.08.027

King, D.A, Davies, S.J, Tan, S, Noor NSMd. (2009). Trees approach gravitational limits to height in tall lowland forests of Malaysia. Functional Ecology 23:284–291

Kolari, P., Lappalainen, H.K., Hänninen, H., & Hari P. (2007). Relationship between temperature and the seasonal course of photosynthesis in Scots pine at northern timberline and in southern boreal zone. Tellus B, 59(3), 542–552. https://doi.org/10.1111/j.1600-0889.2007.00262.x

Kucharik C. J., Norman J. M., Murdock L. M., & Gower S. T. (1997). Characterizing canopy nonrandomness with a multiband vegetation imager (MVI). Journal of Geophysical Research: Atmospheres, 102(D24), 29455–29473. https://doi.org/10.1029/97JD01175

Landsberg, J. J., & Waring, R. H. (1997). A generalised model of forest productivity using simplified concepts of radiation-use efficiency, carbon balance and partitioning. Forest Ecology and Management, 95(3), 209–228.

Landsberg, Joseph John, & Sands, P. J. (2011). Physiological ecology of forest production: principles, processes and models (Vol. 4). Elsevier/Academic Press.

Lawrence, M., McRoberts, R. E., Tomppo, E., Gschwantner, T., & Gabler, K. (2010). Comparisons of National Forest Inventories. In National Forest Inventories (pp. 19–32). Springer, Dordrecht. https://doi.org/10.1007/978-90-481-3233-1_2

Leblanc, S. G., Chen, J. M., Fernandes, R., Deering, D. W., & Conley, A. (2005). Methodology comparison for canopy structure parameters extraction from digital hemispherical photography in boreal forests. Agricultural and Forest Meteorology, 129(3), 187–207. https://doi.org/10.1016/j.agrformet.2004.09.006

Lertzman Kenneth P., Sutherland Glenn D., Inselberg Alex, & Saunders Sari C. (1996). Canopy Gaps and the Landscape Mosaic in a Coastal Temperate Rain Forest. Ecology, 77(4), 1254–1270. https://doi.org/10.2307/2265594

Li, Z. (2010). Improved leaf area index estimation by considering both temporal and spatial variations. Retrieved from https://ecommons.usask.ca/handle/10388/etd-08172010-121849

Liu, J., & Pattey, E. (2010). Retrieval of leaf area index from top-of-canopy digital photography over agricultural crops. Agricultural and Forest Meteorology, 150(11), 1485–1490. https://doi.org/10.1016/j.agrformet.2010.08.002

Macfarlane, C., Hoffman, M., Eamus, D., Kerp, N., Higginson, S., McMurtrie, R., & Adams, M. (2007). Estimation of leaf area index in eucalypt forest using digital photography. Agricultural and Forest Meteorology, 143(3), 176–188. https://doi.org/10.1016/j.agrformet.2006.10.013

Mason, E. G., Holmström, E., & Nilsson, U. (2018). Using hybrid physiological/mensurational modelling to predict site index of Pinus sylvestris L. in Sweden: a pilot study. Scandinavian Journal of Forest Research, 33(2), 147–154. https://doi.org/10.1080/02827581.2017.1348539

Mencuccini, M., & Grace, J. (1996). Hydraulic conductance, light interception and needle nutrient concentration in Scots pine stands and their relation with net primary productivity. Tree Physiology, 16, 459 - 468

Monteith, J. L., & Unsworth, M. H. (2008). Microclimatology of radiation (iii) interception by plants and animals. Principles of Environmental Physics, 116–133.

Nilson, T. (1971). A theoretical analysis of the frequency of gaps in plant stands. Agricultural Meteorology, 8, 25–38. https://doi.org/10.1016/0002-1571 (71)90092-6

Pfeifer, M., Lefebvre, V., Gonsamo, A., Pellikka, P. K. E., Marchant, R., Denu, D., & Platts, P. J. (2014). Validating and Linking the GIMMS Leaf Area Index (LAI3g) with Environmental Controls in Tropical Africa. Remote Sensing, 6(3), 1973–1990. https://doi.org/10.3390/rs6031973

Potithep, S., & Yasuoka, Y. (2011). Application of the 3-PG Model for Gross Primary Productivity Estimation in Deciduous Broadleaf Forests: A Study Area in Japan. Forests, 2(2), 590–609. https://doi.org/10.3390/f2020590

Propastin, P., & Erasmi, S. (2010). A physically based approach to model LAI from MODIS 250m data in a tropical region. International Journal of Applied Earth Observation and Geoinformation, 12(1), 47–59. https://doi.org/10.1016/j.jag.2009.09.013

Royston, P. (1995). Remark AS R94: A Remark on Algorithm AS 181: The W-test for Normality. Journal of the Royal Statistical Society. Series C (Applied Statistics), 44(4), 547–551. https://doi.org/10.2307/2986146

Shen, L., Li, Z., & Guo, X. (2014). Remote sensing of leaf area index (LAI) and a spatiotemporally parameterized model for mixed grasslands. Int. J. Appl, 4(1).

Stenberg, P., Rautiainen, M., Manninen, T., Voipio, P., & Smolander, H. (2004). Reduced simple ratio better than NDVI for estimating LAI in Finnish pine and spruce stands.

Tibshirani, R., James, G., Witten, D., & Hastie, T. (2013). An introduction to statistical learning-with applications in R. New York, NY: Springer.

Trichon, V., Walter, J.-M. N., & Laumonier, Y. (1998). Identifying spatial patterns in the tropical rain forest structure using hemispherical photographs. Plant Ecology, 137(2), 227–244. https://doi.org/10.1023/A:1009712925343

van Gardingen, P. R., Jackson, G. E., Hernandez-Daumas, S., Russell, G., & Sharp, L. (1999). Leaf area index estimates obtained for clumped canopies using hemispherical photography. Agricultural and Forest Meteorology, 94(3), 243–257. https://doi.org/10.1016/S0168-1923 (99)00018-0

Wang, Q., Tenhunen, J., Granier, A., Reichstein, M., Bouriaud, O., Nguyen, D., & Breda, N. (2004). Long-term variations in leaf area index and light extinction in a Fagus sylvatica stand as estimated from global radiation profiles. Theoretical and Applied Climatology, 79(3–4), 225–238.

Waring, R., Landsberg, J., & Linder, S. (2016). Tamm Review: Insights gained from light use and leaf growth efficiency indices. Forest Ecology and Management, 379, 232–242. https://doi.org/10.1016/j.foreco.2016.08.023

Weiss, M., Baret, F., Smith, G. J., Jonckheere, I., & Coppin, P. (2004). Review of methods for in situ leaf area index (LAI) determination: Part II. Estimation of LAI, errors and sampling. Agricultural and Forest Meteorology, 121(1), 37–53. https://doi.org/10.1016/j.agrformet.2003.08.001

Welles, J. M., & Norman, J. M. (1991). Instrument for Indirect Measurement of Canopy Architecture. Agronomy Journal, 83(5), 818–825. https://doi.org/10.2134/agronj1991.00021962008300050009x

West PW. (2014). 2nd edition Growing plantation forests. ISBN 978-3-319-01827-0 ebook.

Yoder, B. J., Ryan, M.G., Waring, R.H., Schoettle, A.W., Kaufmann, M.R. (1994). Evidence of reduced photosynthetic rates in old trees. Forest Science, 40, 513 - 427

Zhang, Y., Chen, J. M., & Miller, J. R. (2005). Determining digital hemispherical photograph exposure for leaf area index estimation. Agricultural and Forest Meteorology, 133(1), 166–181. https://doi.org/10.1016/j.agrformet.2005.09.009

Zheng, G., & Moskal, L. M. (2009). Retrieving Leaf Area Index (LAI) Using Remote Sensing: Theories, Methods and Sensors. Sensors, 9(4), 2719–2745. https://doi.org/10.3390/s90402719